DEVELOPMENT OF SEISMIC COUNTERMEASURES AGAINST CLIFF EDGES FOR ENHANCEMENT OF COMPREHENSIVE SAFETY OF NUCLEAR POWER PLANTS
PART 2: CLIFF EDGES RELEVANT TO NPP STRUCTURE MODELING

Akemi Nishida[1], Byunghyun Choi[2], Hidemasa Yamano[1] and Tsuyoshi Takada[3]

[1] Principal Researcher, Japan Atomic Energy Agency, Japan
[2] Post-doctoral Fellow, Japan Atomic Energy Agency, Japan
[3] Professor, Department of Architecture, The University of Tokyo, Japan

ABSTRACT

This study identified and quantified possible cliff edge effects through a seismic safety evaluation of a nuclear power plant, based on the concepts of risk and defense in depth. Cliff edges of the both physical and knowledge-based type were considered in this study. We investigated a seismic isolation effect, etc., for physical cliff edges, and the modeling of the target structure, boundary conditions, etc., for knowledge-based cliff edges.

Response analysis was performed using a sway-rocking (SR) model and a three-dimensional model of the target building. The seismic isolation effect of the base-isolated building was confirmed by comparison to the results of earthquake-resistant building. In the case of a collision with the retaining wall of the base-isolated building, the level of damage was found to depend on the modeling of the collision condition assumed. On the other hand, the study confirmed the differences between the results from the SR model and the three-dimensional model. And the greater fidelity of the three-dimensional model was also confirmed. This paper presents and discusses these results.

INTRODUCTION

In this study, the seismic safety of nuclear power plants (NPP) was addressed by identifying and quantifying a range of cliff edge effects, based on the concepts of risk and defense in depth. We first attempted to identify the relevant cliff edge effects and devised a methodology for avoiding them. A preliminary elastic–plastic analysis of the NPP building system was performed to model the factor dependence of the cliff edge effects. Next, we performed a preliminary fragility evaluation of the reactor vessel and piping. It was found that the introduction of a seismic isolation system was an effective way of avoiding the cliff edge of the NPP building system and equipment/piping system.

In this paper, we discuss the issues relevant to the cliff edges in an NPP building system. To examine the dependency of the cliff edge state on the modeling factors specified in the seismic response analysis of the building system, we investigated a seismic isolation mechanism and the modeling of boundary conditions for events such as a collision with the retaining wall. This study outlines and discusses our results.

TWO TYPES OF CLIFF EDGE

In this study, cliff edges of the both physical and knowledge-based type were considered (Takada, 2017). Table 1 gives examples of the cliff edges assumed for the building system. We first focused on the cliff edge in a base-isolated building system.

Table 1. Examples of cliff edges assumed for the building system

Physical Cliff Edge	Knowledge-derived cliff edge
Damage to plant building/equipment, foundation lifting, sliding, nonlinear effects, collision with retaining wall of base-isolated building, etc.	Behavior in non-target region of modeling, behavior in region where knowledge and experience are insufficient, e.g., a strongly nonlinear region.

CLIFF EDGES OF A BASE-ISOLATED BUILDING SYSTEM

The cliff edges of a base-isolated building are modeled in Figure 1. The introduction of a seismic isolation system greatly reduces the building response, and it is expected that the physical cliff edge of a normal earthquake-resistant building is avoided. Moreover, the behavior of the base-isolated building stays within the linear elastic region at levels of input ground motion that produce nonlinear behavior in an earthquake-resistant building. The elastic design of equipment then becomes possible, improving the accuracy of design evaluation. Examples of the physical cliff edges of a base-isolated building include damage to the base-isolation device and collision with the retaining wall. Our seismic response analysis of the base-isolated building assumed that these events occurred.
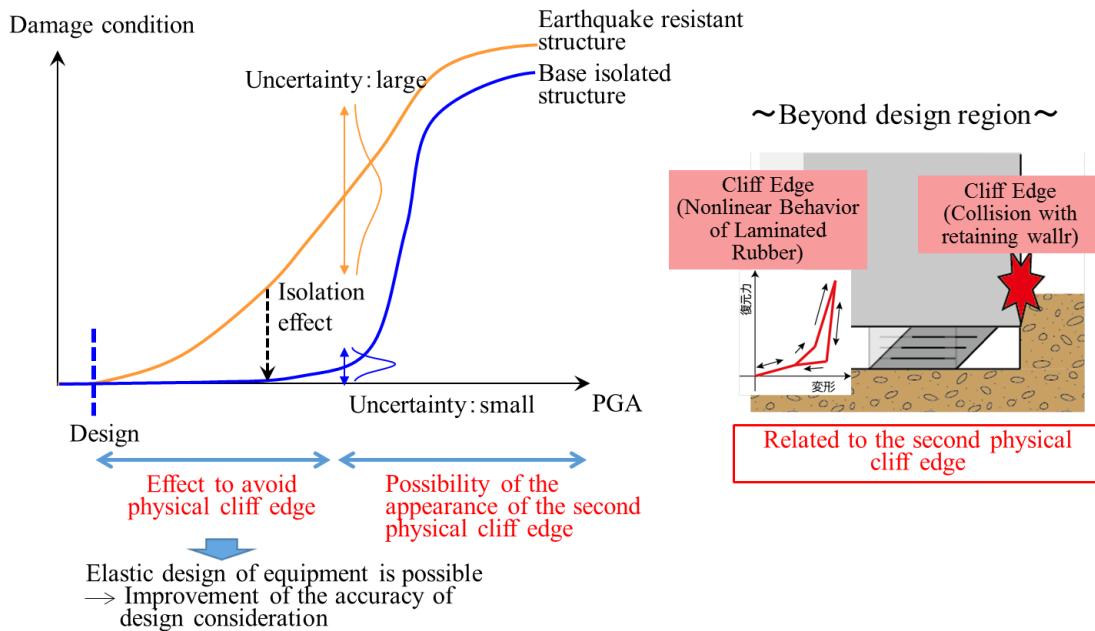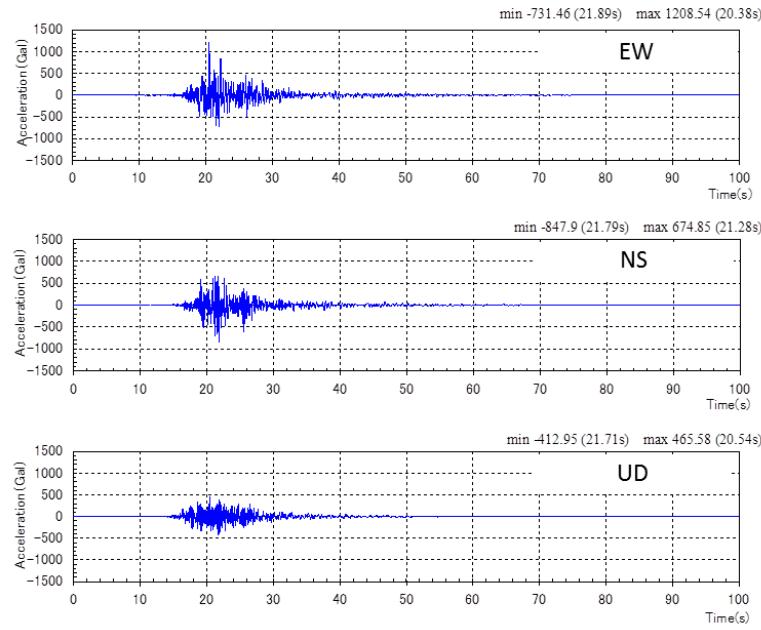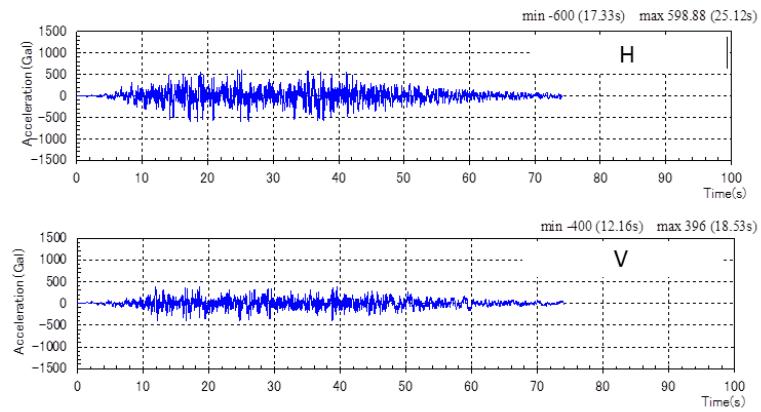

Figure 1. Concept of cliff edge for the base-isolated building system

INPUT GROUND MOTION

As shown in Figure 2, two types of simulated ground motion were used as inputs. Figure 3 shows the acceleration response spectra. Ground motion A comprised a wave generated using a fault model, whereas the wave in ground motion B was generated using a response spectrum method. The maximum acceleration of each wave was based on the basic earthquake ground motion level (before 2010 in Japan). The numerical values are given in Table 2.

(a) Input ground motion A (three axes)

(b) Input ground motion B (H-V2 axes)
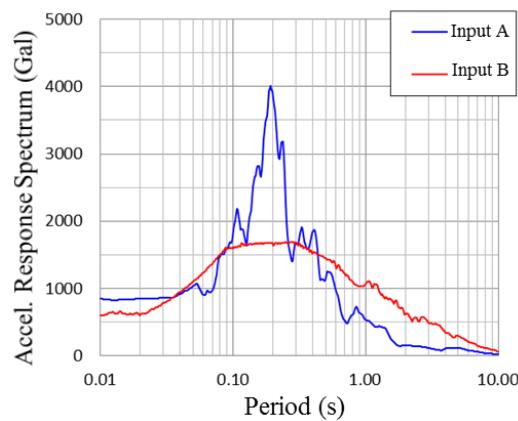Figure 2. Input ground motion used in the analysis

Figure 3. Acceleration response spectrum

Table 2. Maximum acceleration of input ground motion

Input ground motion	Horizontal		Vertical
	EW	NS	UD
A	1209	848	466
B	600		400

ANALYSIS CONDITIONS

Table 3 shows the conditions assumed for the analysis of the cliff edge effect of base-isolated building. For comparison, analyses were also performed for an earthquake-resistant building model. Seismic response analysis was performed on two types of input ground motion. Figure 4 shows an example of an analysis model of a base-isolated building. Figure 4(a) shows the conventional sway-rocking (SR) model, and Figure 4(b) shows the three-dimensional model. Figure 5 shows the hysteresis characteristics of the seismic isolation device, and Figure 6 shows its arrangement within the three-dimensional model. The seismic isolation hysteresis characteristic of the SR model and the three-dimensional model were defined as the normal bilinear model equivalent to the hysteresis characteristics of a lead rubber bearing (LRB). The properties of the seismic isolation device were set referring Asahara (2016) and Shima (2016).

Table 3. Analytical conditions for cliff edge analysis of base-isolated building

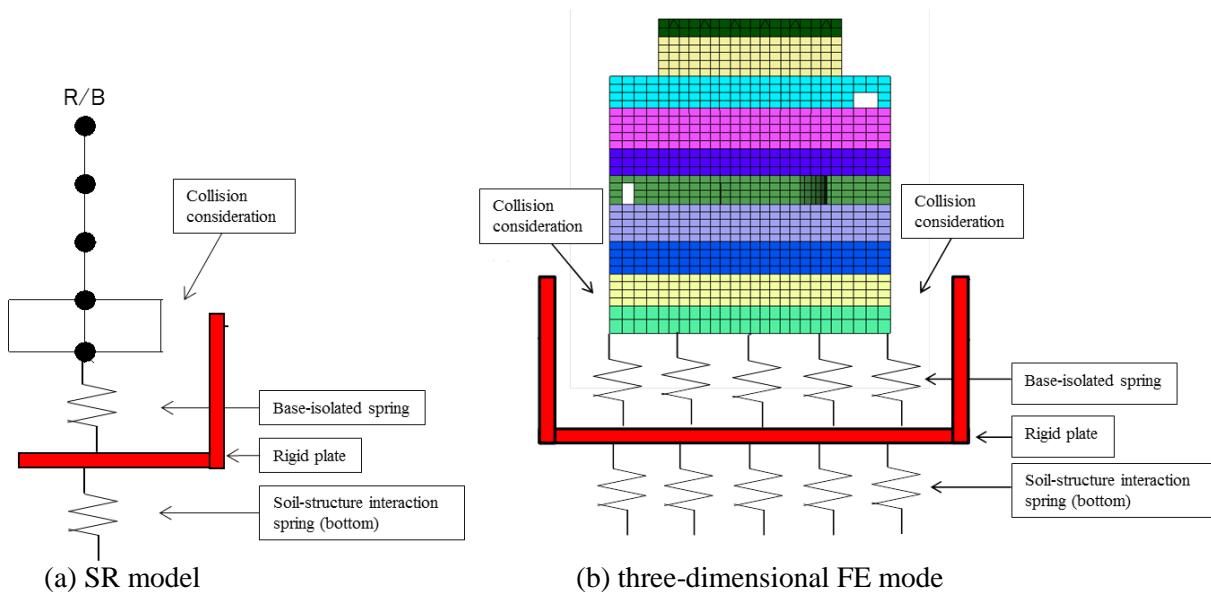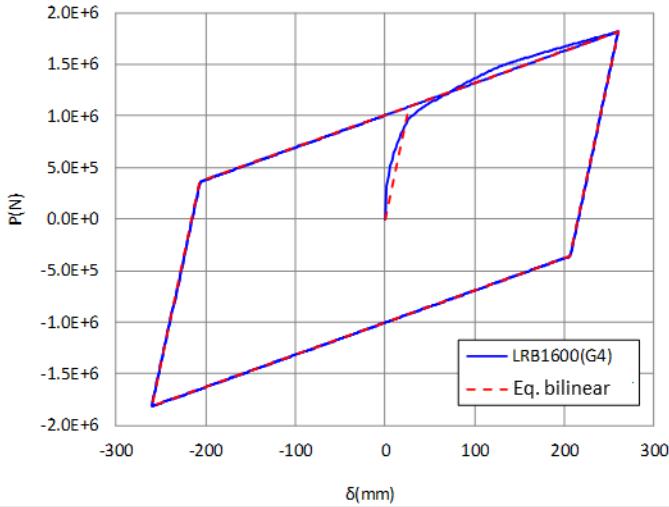|	
Model type	SR mode/three-dimensional model
Embedded effect	Considered/Not considered
Isolation effect	Base-isolated/Earthquake-resistant (not isolated)
Collision with retaining wall	Considered/Not considered
Input wave	Input ground motion A/Input ground motion B
Input direction	N–S
Input magnification	Original wave × 1, 2, 3

(a) SR model   (b) three-dimensional FE mode

Figure 4. Analytical model of a base-isolated building

Initial rigidity of base-isolation device	K_u	40591	N/mm
Yield load of lead plug	Q_d	1005326	N
Yield Load for bilinear curve	Q_y	1089194	N
Gradient rate	α	0.077	-

$$Q_d = CQ_d \times \sigma_{pd} \times A_p$$
$$Q_y = Q_d \times (1 - \alpha)$$

where, CQ_d : Strain-dependent correction factor (1.0 in case of $\gamma \geq 0.5$)
σ_{pd} : Yield shear stress of lead (8.33 N/mm²)
A_p : Cross sectional area of lead plug

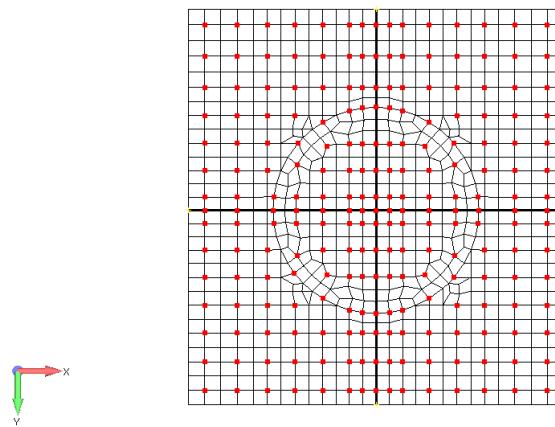Figure 5. The hysteresis characteristics of the seismic isolation device

Figure 6. Arrangement image of the isolation spring under the basemat of the building
(●: a position where the isolation spring is attached)

For setting the nonlinear properties of the reinforced concrete in the three-dimensional model, the Maekawa model was used for the shell elements of the earthquake-resistant wall and the auxiliary wall, and the peak pressure strain was set to 3000 μ so that the initial inclination was equal to the Young's

modulus. A single layer shell element was assumed for nonlinear analysis. A non-orthogonal four-direction crack model was used. The adhesion coefficient of the rebar was set to C = 1.0, based on the rebar-to-shell element ratio. The damping of the three-dimensional model was set using the stiffness proportional approach and was set to 5% at the second natural frequency of the SR model. Table 4 shows the material properties of the concrete and rebar. The stress–strain relations within the Maekawa model are shown in Figures 7 and 8.

Table 4. Material properties of concrete and rebar

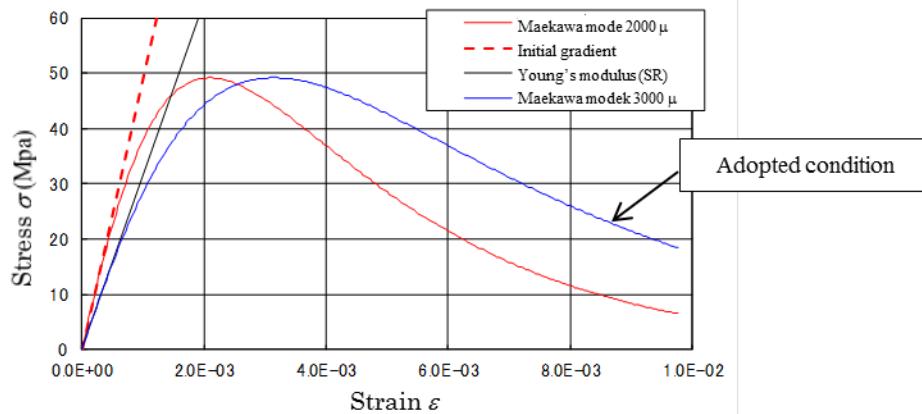| Concrete				Rebar	
Compressive strength F_c N/mm²	Tensile strength σ_{cr} N/mm²	Poisson's ratio υ	Young's modulus E_c N/mm²	Yield point σ_y N/mm²	Young's modulus E_s N/mm²
49.0	3.08	0.2	3.13 E + 04	235	205000

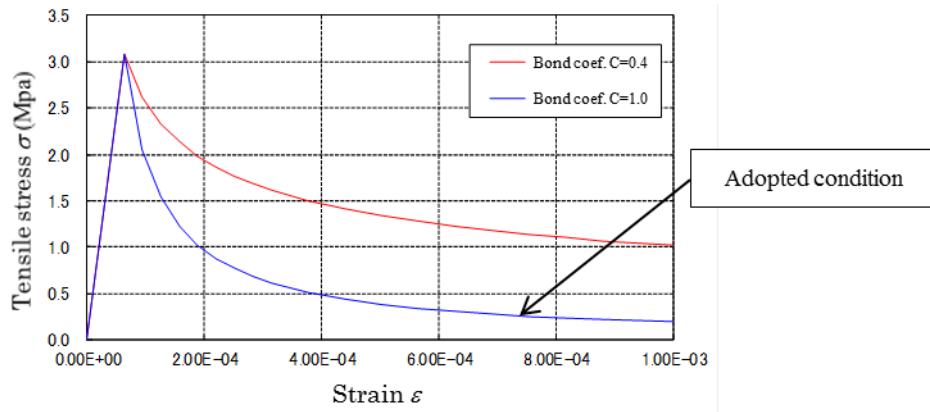Figure 7. Stress–strain relation curve of the Maekawa model (compression side)

Figure 8. Tension stiffening by adhesion parameter C (tension side)

ANALYTICAL RESULTS

Analytical results from SR model

Response analysis of the SR model was performed using input ground motions A and B. The detailed analytical results were given in MEXT (2016). Figures 9 and 10 compare the results for the earthquake-resistant building and the base-isolated building. Boxes (a) and (b) in the two figures confirm the effect of seismic isolation. When the input ground motion comprises multiple long-period components, as that in ground motion B, the horizontal displacement of the isolation system is known to become excessive, increasing the risk of collision with the retaining wall. When this occurred, large local shear strains were generated, as shown in Figure 10(c). The response at the time of the collision was found to be strongly dependent on the rigidity of the collision spring used in the simulation. Therefore, we analyzed the effect of changing the rigidity of the collision spring as a preliminary approach to avoiding the cliff edge. The fragility assessment may reflect the differences in the response caused by factors such as the periodic components of the ground motion or the model settings at the time of the collision. These differences may produce a knowledge-based cliff edge. The floor responses obtained were used to conduct fragility assessments of installed equipment such as piping, though this is not reported here.
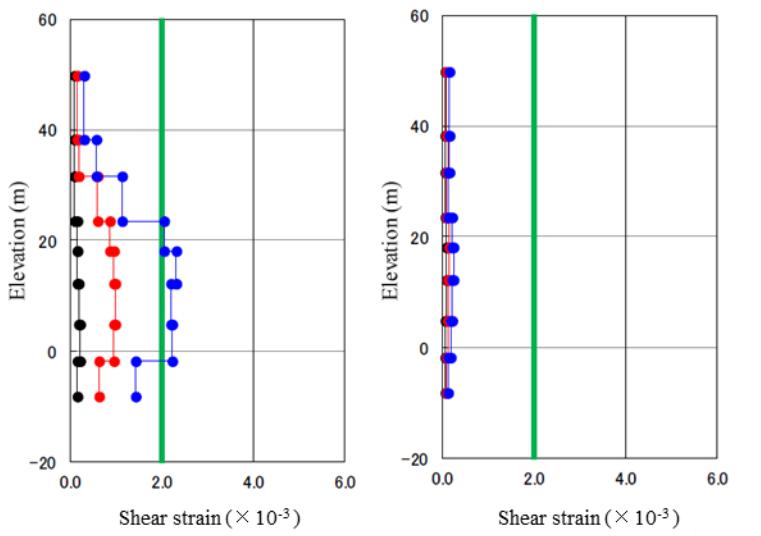

(a) Earthquake-resistant   (b) Base-isolated (no collision)
Figure 9. Shear strain distribution (Input ground motion A)

(a) Earthquake-resistant   (b) Base-isolated (no collision)   (c) Base-isolated (with collision)
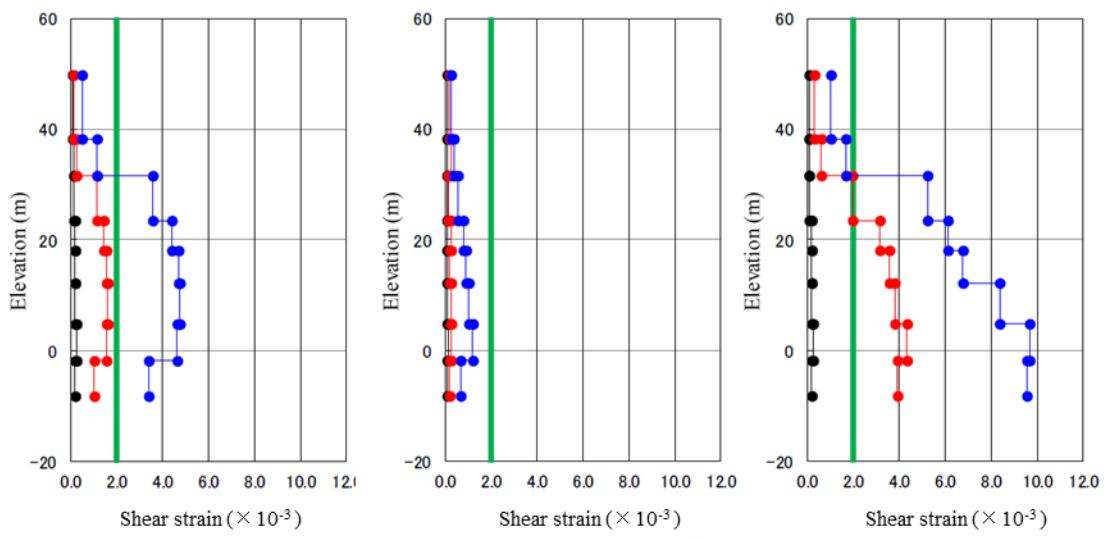Figure 10. Shear strain distribution (Input ground motion B)

Comparison of analytical results from the SR model and three-dimensional model

Figure 11 shows the distribution of the maximum N–S shear strain under ground motion A from the SR model and the three-dimensional model. The shear strain remained within the allowable range at the original load, and the results from the SR model were close to the median value of those obtained from the three-dimensional model. In the floor responses below the first floor of the building, the median value of the results obtained from the three-dimensional model was confirmed to be lower than that from the SR model. However, out-of-plane deformation of the wall under the roof truss of the building increased the shear strain on the wall perpendicular to the deformed wall on the upper floor of the building. This is shown in Figure 12. The results confirmed that the median value from a three-dimensional model is larger than that from an SR model. This suggests that a knowledge-based cliff edge may arise when the evaluation is conducted using an SR model, as the three-dimensional effect is not considered.
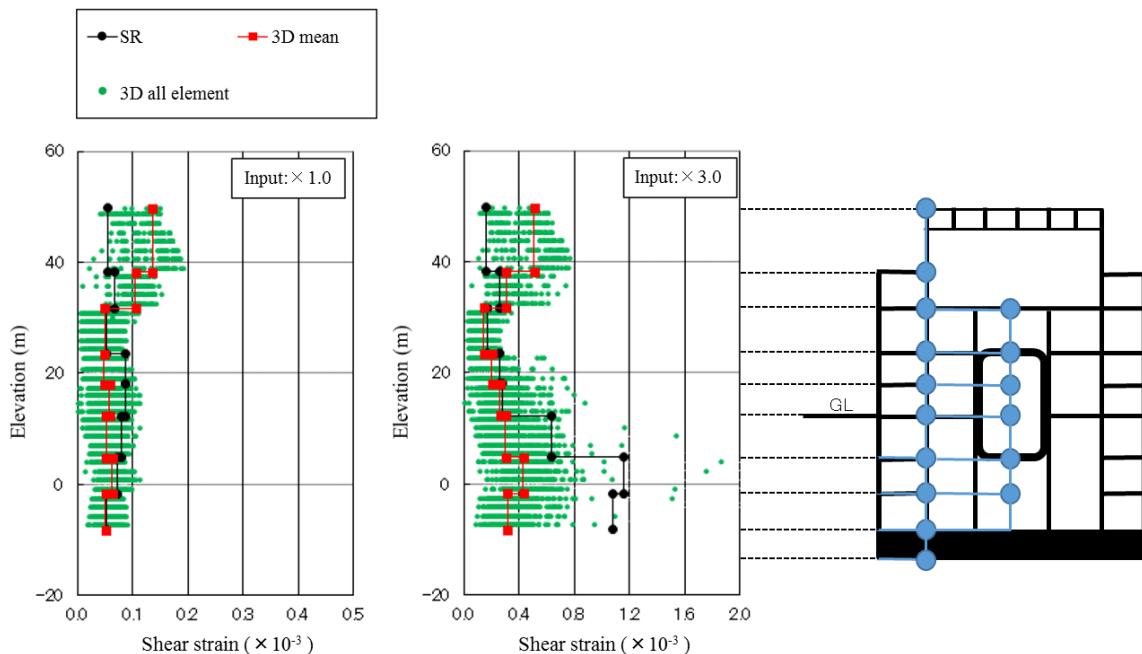

Figure 11. Maximum shear strain from SR model and three-dimensional model.
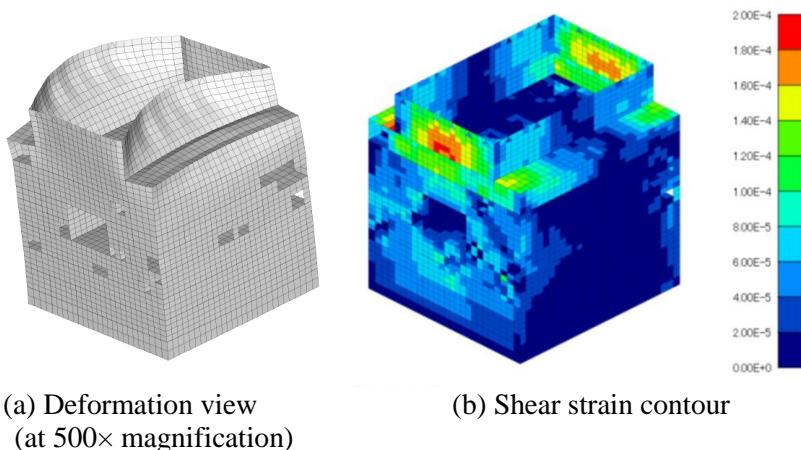Input ground motion A (N–S)

(a) Deformation view   (b) Shear strain contour
(at 500× magnification)
Figure 12. Shear strain distribution in the upper wall of the building (MEXT (2016))

CONCLUSIONS

This study identified and quantified the possible cliff edges in NPP building systems. Cliff edges of the both physical and knowledge-based type were considered in this study. We also created a preliminary study of ways to avoid the identified cliff edges.

Response analysis was performed to identify potential physical cliff edges in a base-isolated building and to explore the effect of base-isolation in reducing the response. The seismic isolation effect of the base-isolated building was confirmed by comparison to the results of earthquake-resistant building. The response of base-isolated building was found to be strongly dependent on the periodic component that was assumed in the input ground motion. In the case of a collision with the retaining wall of the base-isolated building, the level of damage was found to depend on the modeling of the collision condition assumed.

On the other hand, A potential knowledge-based cliff edge was identified in the spatial distribution of the responses of the building walls. This is not considered in the conventional SR model but can be quantified using a three-dimensional model. The study confirmed the differences between the results from the SR model and the three-dimensional model, and the greater fidelity of the three-dimensional model was also confirmed.

In a future study, we intend to further explore techniques for avoiding the cliff edge effects identified here.

ACKNOWLEDGMENTS

REFERENCES

Takada, T., et al. (2017). "Development of Seismic Countermeasures Against Cliff Edges for Enhancement of Comprehensive Safety of NPPs - Part 1: Conceptual Study on Identification and Avoidance of Cliff Edges of NPPs Against Earthquakes", *Proc., SMiRT-24*, Busan, Korea.

The Ministry of Education, Sports, Science and Technology (MEXT), (2016), "Development of Seismic Countermeasures against Cliff Edges for Enhancement of Comprehensive Safety of Nuclear Power Plants", The research report of FY2016, The Initiatives for Atomic Energy Basic and Generic Strategic Research, The Center of World Intelligence Project for Nuclear S&T and Human Resource Development, (in Japanese).

Asahara, S., et al. (2016), "Development of seismic isolation technology for nuclear plant - Part 33: Overview of developments - Part 2: Design and Evaluation of Seismic Isolation Building", Summaries of technical papers of annual meeting, Architectural Institute of Japan, (in Japanese).

Shima T., et al. (2016), "Development of seismic isolation technology for nuclear plant - Part 34: Overview of developments - Part 3: Residual Risk Assessment", Summaries of technical papers of annual meeting, Architectural Institute of Japan, (in Japanese).